IEEE Access
Multidisciplinary | Rapid Review | Open Access Journal

Received 4 November 2022, accepted 2 December 2022, date of publication 7 December 2022,
date of current version 13 December 2022.

Digital Object Identifier 10.1109/ACCESS.2022.3227444

METHODS

Three Steps Toward Low-Complexity: Practical Interference Management in NOMA-Based mmWave Networks

JOONPYO HONG[1], (Student Member, IEEE), PILDO YOON[1], (Student Member, IEEE), SUYOUNG AHN[1], (Student Member, IEEE), YUNHEE CHO[2], JEEHYEON NA[2], (Member, IEEE), AND JEONGHO KWAK[1], (Member, IEEE)

[1]Department of Electrical Engineering and Computer Science, DGIST, Daegu 42988, South Korea
[2]Intelligent Small Cell Research Center, ETRI, Daejeon 34129, South Korea

Corresponding author: Jeongho Kwak (jeongho.kwak@dgist.ac.kr)

This work was supported by the Institute of Information & Communications Technology Planning & Evaluation (IITP) funded by the Korean Government (MSIT) through the 5G Open Intelligence-Defined RAN (ID-RAN) Technique Based on 5G New Radio under Grant 2018-0-01659.

ABSTRACT Beamforming, user scheduling and transmit power on existing interference management schemes in multi-cell mmWave networks have been independently controlled due to the high computational complexity of the problem. In this paper, we formulate a long-term utility maximization problem where beam activation, user scheduling and transmit power are incorporated in a single framework. To develop a low-complex algorithm, we first leverage the Lyapunov optimization framework to transform the original long-term problem into a series of slot-by-slot problems. Since the computational complexity to optimally solve the slot-by-slot problem is even significantly high like existing schemes, we decompose the problem into two different time scales: *(i)* a subproblem to find beam activation probability with a long time-scale and *(ii)* a subproblem to find user scheduling and power allocation with a short time-scale. Moreover, we introduce two additional gimmicks to more simplify the problem: *(i)* sequentially making decisions of beam activation, user scheduling, and power allocation, and *(ii)* considering a critical user for power allocation. Finally, via extensive simulations, we find that the proposed CRIM algorithm outperforms existing algorithms by up to 47.4% in terms of utility.

INDEX TERMS Beam ON/OFF scheduling, user scheduling, power allocation, inter-beam interference, Lyapunov optimization.

I. INTRODUCTION

As UHD (Ultra High Definition) video streaming or MR (Mixed Reality) services have been emerging as killer applications in 5G+/6G, mobile data traffic has been drastically increasing [1]. To cope with such exploding traffic, various communication technologies such as massive MIMO (Multiple Input Multiple Output) [2], CoMP (Cooperative MultiPoint) [3], UDN (Ultra Dense Networks) [4], and NOMA (Non-Orthogonal Multiple Access) [5] have been recently developed. Besides, mmWave has been regarded as a promising frequency band for future communication systems thanks to its significantly wide bandwidth. On the other hand, mmWave has a limited range and is susceptible to blockage due to its high frequency and short wavelength characteristics. Consequently, mmWave communication for long-distance cellular access is problematic, but it provides a great opportunity for small cells aiming to support short-range communication with high traffic demand [6].

Reducing cell size (equivalently, deploying more BSs (Base Station)) can be one of the ways to enhance the entire network throughput in the same area. However, such a small cell network is likely to increase both the strength and the variation of the inter-cell interference due to the shorter

The associate editor coordinating the review of this manuscript and approving it for publication was Adao Silva.

distance between cells and more heterogeneous cell deployment [7]. Accordingly, an efficient and adaptive inter-cell (and intra-cell) interference mitigation policy must be devised to improve the network throughput.

There have been many studies on IM (Interference Management) in a multi-cell single antenna system [8], [9]. Since the utility maximization problem to jointly make decisions of transmit power and user scheduling for all BSs is an MINLP (Mixed-Integer NonLinear Programming), most studies focused on the development of approximation algorithms by reducing the computational complexity. For example, Xiao et al. [8] proposed an algorithm based on the game theory where each BS belongs to more than one cluster, and considered only intra-cluster interference to make decisions of user scheduling and transmit powers. Moreover, Liu et al. [9] managed interference by decomposing it into cross-tier/co-tier interference to reduce the complexity and by allocating resources separately for utility maximization.

Meanwhile, as an enhanced interference mitigation technique, the MIMO system was proposed to form a directional beam which can focus the signal on a specific point so that it reduces the loss of the spreading signal [2]. Thanks to this advantage, many IM schemes on top of the MIMO system have been proposed [10], [11]. However, although the MIMO system can mitigate the inter-cell interference significantly, joint optimization of beamforming, user scheduling and transmit power control has high computational complexity. Therefore, there have been many studies on the development of low-complex and practical algorithms rather than theoretically-optimal algorithms [10], [11]. For example, Cui et al. [10] proposed a joint user scheduling and power control algorithm with ORBF (Orthogonal Random BeamForming) technique to reduce the computational complexity where the solution strikes a good computational complexity-optimality trade-off by exploiting the matching theory and successive convex approximation techniques. Moreover, Song et al. [11] proposed a multi-beams prioritized transmit power allocation algorithm to guarantee the QoS (Quality of Service) of users and improve the achievable data rate while intra-cell interference is ignored for low complexity.

One step further, by incorporating NOMA in the MIMO system, it is possible to schedule more than two users in the same beam thanks to SC (Superposition Coding) and SIC (Successive Interference Cancellation) so that the sum capacity for one beam can be increased [13]. There have been a few works to address IM on top of this NOMA-based MIMO system [14], [15]. For example, Fang et al. [15] proposed a two-side matching theory-based subchannel assignment and power control algorithm where the objective is to maximize energy efficiency. *However, they assumed that the number of allocated users for one beam is up to two users.*

Although they provided several IM solutions to enhance the system performance, the existing works in small cell systems have two obstacles as follows: *(i)* The number of BSs to be managed by one BS controller gets higher as the cell size becomes smaller; hence more low-complexity IM is required. *(ii)* The inter-cell interference becomes higher due to the shorter distance between cells; hence more efficient transmit power management is required. To overcome these obstacles, we exploit features of future network as follows.

Future 6G networks are likely not only to be reluctant to manage a lot of BSs in a single BS controller due to the reduced cell size but also pervasively deploy the MEC (Multi-access Edge Computing) servers attached to BSs [16]. Hence, the hierarchical cellular architecture is expected where one MEC server manages a small number of physically close BSs whereas a cloud server manages such MEC servers with a long time scale as shown in Fig. 1 [17]. A single MEC server can manage a small number of multiple BSs within a short range (e.g., 1km radius of the circle) via a rapid fronthaul interface (e.g., X2 interface [18]); hence it would be possible to share the parameters required for cellular operations in real-time. Moreover, since a smart grid system is known to be able to measure the power usage and manage the power supply in real-time within approximately 1km coverage [7], a single MEC server would be able to manage the transmit power of BSs in real-time as well. This fact enables an MEC server to manage the long-term transmit power budget, which leads to the flexible adaptation of transmit powers to the spatio-temporally varying interference environment.

Accordingly, in this paper, we propose the *CRIM* (CRitical user based Interference Management) algorithm on top of the future 6G network architecture in which each MEC server controls a small set of BSs in a centralized manner while exchanging the lowest amount of feedback information with each other in a decentralized manner. Specifically, *CRIM* has the following characteristics: *(i)* It reduces the computational complexity by sequentially solving beam activation, user scheduling, and power allocation subproblems. *(ii)* It utilizes the critical user concept, which considers only the highest victim of the interference when making a decision of the transmit power. *(iii)* It spatio-temporally shares the transmit powers of BSs managed by a single MEC server. To this end, we first formulate a long-term utility maximization problem constrained by a time-average transmit power to each MEC server to make decisions of beam activation, user scheduling, and transmit power every time slot. Since the optimal solution of the original problem probably has extremely high computational complexity, we decompose the original problem into two subproblems with different time scales where the solution of the beam activation runs on a slower time scale than that of the user scheduling and transmit power allocation problem. Besides, we apply Lyapunov DMU (Drift-Minus-Utility framework) [19] to the subproblems so that they are solved every time slot without loss of optimality. However, the transformed subproblems are still known as NP-hard; hence we introduce the intuitive idea, namely inner and outer reference users to optimize the transmit power with low computational complexity.

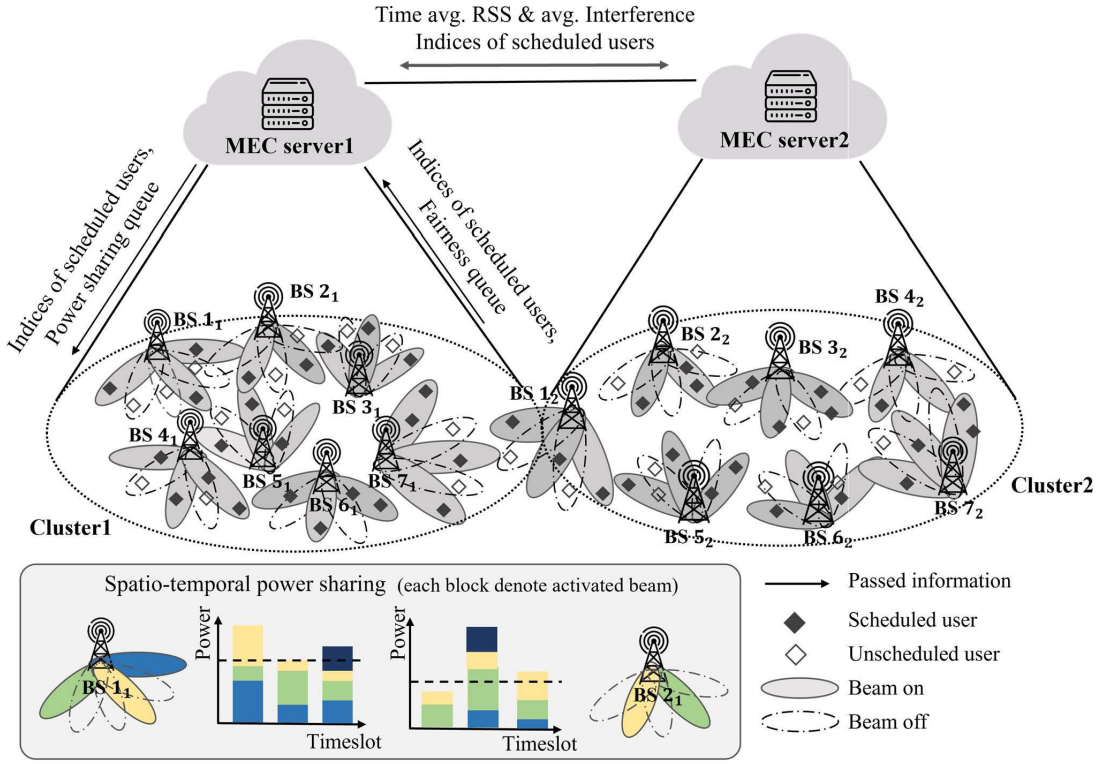

FIGURE 1. An illustration of the considered network architecture.

The contributions of this paper are summarized as follows.

1) We formulate beam selection, user scheduling, and transmit power allocation problems on top of future network architecture with MEC aiming to maximize the time-averaged sum of utilities of users.
2) We propose a low-complex sequential beam selection, user scheduling, and transmit power allocation algorithm, namely *CRIM* where the low-complexity comes from three steps of approximations as follows. The first step is the decomposition of time scales between beam selection and the user scheduling/transmit power allocation. The second step is to cut the loop among the beam selection, user scheduling and transmit power allocation. The third step is to introduce two virtual queues (i.e., power sharing queue and fairness queue) and the critical user concept.
3) Extensive simulations based on the real mmWave standard parameters demonstrate that the proposed *CRIM* algorithm outperforms the existing algorithms up to 47.4% in terms of utility.

In the rest of this paper, we begin with the system model in section II. Next, in Section III, we formulate the optimization problem and propose the CRIM algorithm. Then, in Section IV, we evaluate the CRIM algorithm by extensive simulation. Finally, we conclude this paper in Section V.

II. SYSTEM MODEL

A. NETWORK MODEL

We consider a mmWave small cell network architecture where a small number of BSs are managed by a single MEC server (we call a set of the managed BSs as a cluster) and each MEC server exchanges sparse information among them as shown in Fig. 1. In this architecture, there are C clusters and N BSs where $\mathcal{C} = \{1, \cdots, c, \cdots, C\}$ and $\mathcal{N} = \{1, \cdots, n, \cdots, N\}$ mean the set of clusters and BSs, respectively. Each cluster c has N_c BSs and the set of BSs included in cluster c is denoted by $\mathcal{N}_c = \{1_c, \cdots, n_c, \cdots, N_c\}$. Besides, there are the set of users denoted by $\mathcal{K} = \{1, \cdots, K\}$, and the set of users included in BS n_c are denoted by $\mathcal{K}_{n_c}$. Each BS has to be included in a single cluster, and each user has to be included in a single BS. In the aforementioned system model, each BS has L transmit antennas and each user has a single receive antenna. Hence, BS n can generate up to L precoding vectors $\mathcal{B}_n = \{\boldsymbol{b}_{n,1}, \boldsymbol{b}_{n,2}, \cdots, \boldsymbol{b}_{n,|\mathcal{B}_n|}\}$, [1] $|\mathcal{B}_n| \leq L$ and can schedule multiple users to a precoding vector $\boldsymbol{b} \in \mathcal{B}_n$ by taking advantage of NOMA.[2] Moreover, we consider a time-slotted system where each time slot is indexed by $t \in \{0, 1, \cdots, T-1\}$ and assume a full buffer traffic model meaning that an infinite data packet queue is allocated to all users. This assumption makes each user achieve a different instantaneous data rate based on the time-varying wireless channel

[1] $|\cdot|$ is the cardinality of a set.
[2] In the rest of this paper, we name $\boldsymbol{b}$ as beam.

and the different average data rate. Moreover, achievement of different data rates among users makes users to be scheduled in different beams or the same beam. Consequently, each BS has to make decisions of *(i)* the beams to be activated, *(ii)* the users to be scheduled in the activated beams, and *(iii)* the amount of power to be allocated for each activated beam every time slot.

1) BEAM ACTIVATION

At each time slot t, each BS has to determine which beams are activated. However, exhaustive search of all beams can be a computational burden for the BS when the number of beams is high. To avoid high complexity, we define a set of beam patterns $\mathcal{A}$. It is composed of sets of the activated beams by ensuring that adjacent beams are not activated simultaneously as shown in Fig. 2.[3] Note that this constraint extremely reduces the set of candidates of the activated beams [20]. Hence, each BS selects a set of beam activations a from the predefined set of beam patterns $\mathcal{A}$ every time slot and then activates beams in a. We define $X_{n,a}(t)$ as pattern selection indicator where $X_{n,a}(t) = 1$ means BS n selects a set of beam activations a, and $X_{n,a}(t) = 0$ otherwise. Moreover, we denote $a_n(t)$ as a selected set of beam activations by BS n.

$$\sum_{a\in\mathcal{A}} X_{n,a}(t) = 1, \quad \forall n \in \mathcal{N}. \tag{1}$$

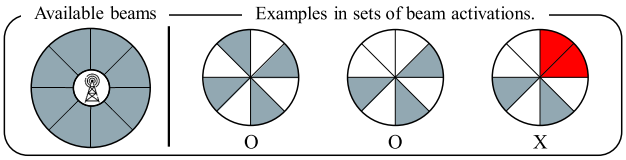

FIGURE 2. Examples of the set of beam activations in $L = 8$.

2) USER SCHEDULING

Once beam activation is decided, users are scheduled to be served by the activated beams. First, we define the user scheduling indicator denoted by $I^k_{n,\boldsymbol{b}}(t)$ where $I^k_{n,\boldsymbol{b}}(t) = 1$ implies that user k is scheduled on beam $\boldsymbol{b}$ of BS n at time slot t, and $I^k_{n,\boldsymbol{b}}(t) = 0$ otherwise. Moreover, since we consider NOMA system, each BS can schedule multiple users on a single beam. To address this, we denote $\mathcal{I}_{n,\boldsymbol{b}}(t) = \{k_1, \cdots, k_{|\mathcal{I}_{n,\boldsymbol{b}}(t)|}\}$ by the set of scheduled users in beam $\boldsymbol{b}$ of BS n. Moreover, we sort $\mathcal{I}_{n,\boldsymbol{b}}(t)$ in descending order for computational convenience in SIC. Then, we have:

$$\sum_{k\in\mathcal{K}} I^k_{n,\boldsymbol{b}}(t) = \left|\mathcal{I}_{n,\boldsymbol{b}}(t)\right|, \quad \forall n \in \mathcal{N}, \quad \forall \boldsymbol{b} \in \mathcal{B}_n. \tag{2}$$

Naturally, beams on which no users are scheduled are deactivated. To represent this, we define $\boldsymbol{b}^{a_n}(t)$ as the set of activated beams where $\boldsymbol{b}^{a_n}(t) \subset a_n(t)$.

[3]Kim et al. [20] showed that activation of neighboring beams affects the highest interference to the main beams.

3) POWER ALLOCATION

In NOMA system, multiple users can be scheduled in the same frequency/time resource; hence different transmit powers are allocated to different users in the resource. Therefore, each BS has to decide the amount of transmit powers to be allocated for scheduled users. We denote by $p^k_{n_c,\boldsymbol{b}}(t)$ the transmit power for user k scheduled on beam $\boldsymbol{b}$ of BS n_c at time slot t, and $p_{n_c,\boldsymbol{b}}(t)$ the transmit power for beam $\boldsymbol{b}$ of BS n_c at time slot t where

$$\sum_{k\in\mathcal{K}} p^k_{n_c,\boldsymbol{b}}(t) = p_{n_c,\boldsymbol{b}}(t), \quad \forall n_c \in \mathcal{N}_c, \quad \forall \boldsymbol{b} \in \mathcal{B}_{n_c}, \quad \forall c \in \mathcal{C}. \tag{3}$$

Then, we define $P^{max}_{n_c}$ and $P^{max}_{n_c,\boldsymbol{b}}$ as the maximum transmit power of a BS and an activated beam, respectively. Accordingly, we have the following power constraints:

$$\sum_{b\in\mathcal{B}_{n_c}} p_{n_c,\boldsymbol{b}}(t) \le P^{max}_{n_c}, \quad \forall n_c \in \mathcal{N}_c, \quad \forall c \in \mathcal{C}, \tag{4}$$

$$p_{n_c,\boldsymbol{b}}(t) \le P^{max}_{n_c,\boldsymbol{b}}, \forall n_c \in \mathcal{N}_c, \quad \forall \boldsymbol{b} \in \mathcal{B}_{n_c}, \quad \forall c \in \mathcal{C}. \tag{5}$$

As mentioned in Section I, real-time transmit power management among inner cluster BSs would be possible via an MEC server in the future 6G networks. Hence, BSs can flexibly allocate transmit powers over time and space with the average power constraint at each cluster as follows:

$$\lim_{T\to\infty} \frac{1}{T} \sum_{t=0}^{T-1} \sum_{n_c\in\mathcal{N}_c} \sum_{\boldsymbol{b}\in\mathcal{B}_{n_c}} p_{n_c,\boldsymbol{b}}(t) \le P^c_{avg}, \quad \forall c \in \mathcal{C}, \tag{6}$$

where P^c_{avg} means the long-term power budget from the network operator.

B. LINK CAPACITY MODEL

Since each BS has L transmit antennas, a channel gain vector $\boldsymbol{h}_{n,k}$ between BS n and user k can be described as follows:

$$\boldsymbol{h}_{n,k}(t) = [\alpha_{n,k,1}(t), \cdots, \alpha_{n,k,L}(t)]\sqrt{\rho_{n,k}} \in \boldsymbol{h}, \tag{7}$$

where $\alpha_{n,k,l}$ means a channel coefficient of each antenna corresponding to BS n, user k, and antenna l and $\rho_{n,k}$ means a large scale fading including path loss and shadowing between BS n and user k.

In NOMA system, user k scheduled on beam $\boldsymbol{b}$ can be interfered by the signal of users scheduled in the same beam $\boldsymbol{b}$, i.e., users in $\mathcal{I}_{n,\boldsymbol{b}}(t)$ who are sorted before user k. Note that the signal of users in $\mathcal{I}_{n,\boldsymbol{b}}(t)$ who are sorted after user k can be ignored thanks to the SC and SIC techniques. Moreover, user k can be interfered by signals of all beams except for beam $\boldsymbol{b}$ of BS n. Consequently, the total interference of user k, $\eta_k(t)$ can be calculated by

$$\eta_k(t) = \sum_{j=1}^{i-1} \left|\sqrt{p^{k_j}_{n,\boldsymbol{b}}}\boldsymbol{h}_{n,k}(t)\boldsymbol{b}\right|^2 + \sum_{m\in\mathcal{N}\setminus n} \sum_{\boldsymbol{f}\in\mathcal{B}_m} \left|\sqrt{p_{m,\boldsymbol{f}}}\boldsymbol{h}_{m,k}(t)\boldsymbol{f}\right|^2$$

$$+ \sum_{\boldsymbol{q}\in\mathcal{B}_n\setminus\boldsymbol{b}} \left|\sqrt{p_{n,\boldsymbol{q}}}\boldsymbol{h}_{n,k}(t)\boldsymbol{q}\right|^2, k_j \in \mathcal{I}_{n,\boldsymbol{b}}(t), \quad (8)$$

where i and j denote index of user k and index of other users in $\mathcal{I}_{n,\boldsymbol{b}}(t)$, respectively. Here, the first term implies the intra-beam interference from users allocated more power than user k. The second term implies interference from other BSs except for BS n. The third term implies interference from activated beams of BS n except for beam $\boldsymbol{b}$. Through this, the SINR of user k, $\mu_k(\boldsymbol{X}(t), \boldsymbol{I}(t), \boldsymbol{p}(t))$ can be expressed:

$$\mu_k(\boldsymbol{X}(t), \boldsymbol{I}(t), \boldsymbol{p}(t)) = \frac{\sum_{n\in\mathcal{N}}\sum_{\boldsymbol{b}\in\mathcal{B}_n}\left|\sqrt{p^k_{n,\boldsymbol{b}}(t)}\boldsymbol{h}_{n,k}(t)\boldsymbol{b}\right|^2 I^k_{n,\boldsymbol{b}}(t)X_{n,a}(t)}{\eta_k(t)+\sigma_k(t)}, \quad (9)$$

where $\sigma_k(t)$ is a thermal noise of user k at time slot t. Here, pattern selection indicator is expressed by $\boldsymbol{X}(t) = (X_{n,a}(t) : \forall n \in \mathcal{N}, \forall a \in \mathcal{A})$, user scheduling indicator is expressed by $\boldsymbol{I}(t) = (I^k_{n,\boldsymbol{b}}(t) : \forall n \in \mathcal{N}, \forall \boldsymbol{b} \in \mathcal{B}_n, \forall k \in \mathcal{K})$, and power allocation vector is expressed by $\boldsymbol{p}(t) = (p^k_{n,\boldsymbol{b}}(t) : \forall n \in \mathcal{N}, \forall \boldsymbol{b} \in \mathcal{B}_n, \forall k \in \mathcal{K})$.

Finally, for given SINR expression (9), we can calculate the achievable data rate of user k by exploiting Shannon's capacity formula [21] as follows:

$$r_k(\boldsymbol{X}(t), \boldsymbol{I}(t), \boldsymbol{p}(t)) = BW \log_2(1 + \mu_k(\boldsymbol{X}(t), \boldsymbol{I}(t), \boldsymbol{p}(t))), \quad (10)$$

where BW denotes the entire system channel bandwidth.

III. PROBLEM FORMULATION AND ALGORITHM DEVELOPMENT

A. PROBLEM FORMULATION

First, we formulate the utility maximization problem in NOMA-based mmWave network system as follows:

$$(\mathbf{P}): \max_{(\boldsymbol{X},\boldsymbol{I},\boldsymbol{p})} \sum_{k\in\mathcal{K}} U_k(R_k)$$
$$s.t. \quad \sum_{a\in\mathcal{A}} X_{n,a}(t) = 1, \quad \forall n \in \mathcal{N},$$
$$(2), (3), (4), (5), (6).$$

Without loss of generality, $U_k(\cdot)$ should be concave, strictly increasing, and continuously differentiable for mathematical convenience [22]. This indicates the degree of user satisfaction with their average throughput (i.e., $R_k = \overline{r_k(\boldsymbol{X}(t), \boldsymbol{I}(t), \boldsymbol{p}(t))}$).[4] In this study, we design the utility function as $U_k(R_k) = \log(1 + R_k)$. This design enables the function to capture both fairness and throughput of users in two ways: *(i)* since the sum of the log function is expressed as a product, similar utility values for different users make the objective bigger (fairness), and *(ii)* thanks to the maximization operation, the utility function becomes higher as each $U_k(\cdot)$ gets larger (throughput).

[4]Note that $\overline{X}$ means the long-term average function of $x(t)$. (i.e., $X = \lim_{T\to\infty}\frac{1}{T}\sum_{t=0}^{T-1} x(t)$) and $\overline{f(X)} = \lim_{T\to\infty}\frac{1}{T}\sum_{t=0}^{T-1}\mathbb{E}\{f(x(t))\}$).

We should note that there are three obstacles to solve the problem **(P)** as follows: *(i)* **(P)** is long-term average utility maximization problem, yet our practical problem is to find beam activation, user scheduling and power allocation every time slot, i.e., online-fashioned solution, *(ii)* finding joint beam activation, user scheduling and power allocation is NP-hard problem, *(iii)* future information on the time-varying wireless channels cannot be known in advance. Hence, we exploit Lyapunov optimization framework [19] to derive practical problem since this well-known dynamic optimization framework does not require the future wireless channel information and the time-average constraints, i.e., average power constraints can be modeled as the operation of virtual queue; hence we can easily interpret the algorithm operation.

As a first step, we separate **(P)** into **(P1)** and **(P-Pattern)**:

$$(\mathbf{P1}): \max_{(\boldsymbol{I},\boldsymbol{p})} \sum_{k\in\mathcal{K}} U_k(R_k),$$
$$s.t. \quad (2), (3), (4), (5), (6).$$
$$(\mathbf{P\text{-}Pattern}): \max_{\boldsymbol{X}} \sum_{k\in\mathcal{K}} U_k(R_k),$$
$$s.t. \quad \sum_{a\in\mathcal{A}} X_{n,a}(t) = 1, \quad \forall n \in \mathcal{N}.$$

Note that **(P1)** and **(P-Pattern)** have the same objective function, yet **(P1)** is the problem to find solutions of user scheduling and power allocation, and **(P-Pattern)** is the problem to find solution of beam activation pattern where time scales for two problems are different.[5]

1) PROBLEM TRANSFORMATION

Since the objective function of **(P1)** is not linear, Lyapunov optimization framework cannot be directly applied in this problem. Hence, to transform **(P1)** into the applicable problem to Lyapunov optimization framework, we introduce a rectangular constraint and ancillary variables. We define a rectangle set $\Gamma = \{(\gamma_1, \ldots, \gamma_K) \mid \gamma_{k,min} \le \gamma_k \le \gamma_{k,max}, \forall k \in \mathcal{K}\}$ and the ancillary variable $\boldsymbol{\gamma}(t) = (\gamma_1(t), \cdots, \gamma_K(t)) \in \boldsymbol{\Gamma}$, where $\gamma_{k,min}$ and $\gamma_{k,max}$ are any constraints and the ancillary variable $\boldsymbol{\gamma}(t)$ follows $\boldsymbol{r}(t)$ smoothly over time. Leveraging Jensen's inequality [19], we can reformulate the problem **(P1)** to **(P2)** as follows:

$$(\mathbf{P2}): \max_{(\boldsymbol{I},\boldsymbol{p},\boldsymbol{\gamma})} \sum_{k\in\mathcal{K}} \overline{U_k(R_k)}$$
$$s.t. \quad (2), (3), (4), (5), (6),$$
$$\overline{\gamma_k} \le R_k, \quad \forall k \in \mathcal{K}, \quad (11)$$
$$\boldsymbol{\gamma}(t) \in \boldsymbol{\Gamma}, \quad \forall t \in \mathcal{T}. \quad (12)$$

where $\boldsymbol{\gamma} = \{\boldsymbol{\gamma}(t) : t \in \mathcal{T}\}$. To capture constraints (6) and (11) in per-slot problem, we add two virtual queues $Z_c(t)$ for each cluster and $W_k(t)$ for each user.[6] Here, two virtual queues

[5] **(P1)** should be solved in every time slot whereas **(P-Pattern)** should be solved in a longer time scale, e.g., 100 time slots.

[6]Note that stabilizing two virtual queues implies guaranteeing the time-average constraints (6) and (11).

evolve according to the following equations:

$$Z_c(t+1) = [Z_c(t) - P_{avg}^c + \sum_{n_c \in \mathcal{N}_c} \sum_{\boldsymbol{b} \in \mathcal{B}_{n_c}} p_{n_c,\boldsymbol{b}}(t)]^+, \quad \forall c, \tag{13}$$

$$W_k(t+1) = [W_k(t) - r_k(\boldsymbol{I}(t), \boldsymbol{p}(t)) + \gamma_k(t)]^+, \quad \forall k, \tag{14}$$

where two queues are initialized by finite backlogs, i.e., $Z_c(0), W_k(0) < \infty$.[7] Next, we define Lyapunov function $L(t)$ as follows:

$$L(\boldsymbol{Q}(t)) = \frac{1}{2}\Big\{ \sum_c Z_c^2(t) + \sum_k W_k^2(t) \Big\}, \tag{15}$$

where $\boldsymbol{Q}(t) = (W_1(t), \ldots W_K(t); Z_1(t), \ldots, Z_C(t))$. Then, by utilizing the above Lyapunov function, the drift function $\Delta L(\boldsymbol{Q}(t))$ can be designed as follows:

$$\Delta L(\boldsymbol{Q}(t)) = \mathbb{E}\{L(\boldsymbol{Q}(t+1)) - L(\boldsymbol{Q}(t))\}. \tag{16}$$

Then, we design a Lyapunov DMU function, which makes a single objective function which captures both objective function and virtual queue stability in every time slot as follows:

$$\begin{aligned} &\text{DMU}(\boldsymbol{p}(t), \boldsymbol{I}(t), \boldsymbol{\gamma}(t)) \\ &= \Delta L(\boldsymbol{Q}(t)) - V \sum_c \sum_{n_c} \sum_k \mathbb{E}\{\log(1+\gamma_k(t)) | \boldsymbol{Q}(t)\}. \end{aligned} \tag{17}$$

Then, we derive the upper bound of DMU function (17) using queueing dynamics equations (13) and (14) and the objective function as follows:

$$\begin{aligned} &\text{DMU}(\boldsymbol{p}(t), \boldsymbol{I}(t), \boldsymbol{\gamma}(t)) \\ &\le B - V \sum_k \mathbb{E}\{\log(1+\gamma_k(t)) | \boldsymbol{Q}(t)\} \\ &\quad - \sum_c \mathbb{E}\{(P_c^{avg} - \sum_{n_c} \sum_{\boldsymbol{b}} p_{n_c,\boldsymbol{b}}(t)) Z_c(t) | \boldsymbol{Q}(t)\} \\ &\quad - \sum_k \mathbb{E}\{(r_k(\boldsymbol{p}(t), \boldsymbol{I}(t)) - \gamma_k(t)) W_k(t) | \boldsymbol{Q}(t)\}, \end{aligned} \tag{18}$$

where $B = \frac{1}{2}(K(r_{k,max}^2 + \gamma_{k,max}^2) + \sum_c N_c \boldsymbol{B} P_{n_c,max}^2 + C P_{c,max}^2)$. Then, by minimizing the RHS (Right-Hand-Side) in (18) every slot, an optimal objective value in (**P2**) can be obtained [19]. Then, the minimization problem of RHS in (18) can be decomposed into two subproblems as follows:

(SP1) Problem to find optimal $\gamma_k^*(t)$:

$$\max_{\gamma_k(t)} V \log(1+\gamma_k(t)) - \gamma_k(t) W_k(t), \quad \forall k \in \mathcal{K},$$

(SP2) Problem to find optimal $\boldsymbol{I}^*(t)$ and $\boldsymbol{p}^*(t)$:

$$\max_{(\boldsymbol{I}(t), \boldsymbol{p}(t))} \sum_{k \in \mathcal{K}} r_k(\boldsymbol{I}(t), \boldsymbol{p}(t)) W_k(t) - \sum_{n_c \in \mathcal{N}_c} \sum_{\boldsymbol{b} \in \mathcal{B}_{n_c}} p_{n_c,\boldsymbol{b}}(t) Z_c(t), \quad s.t. \ (4), (5), (6).$$

[7] When running the simulation in this study, both $Z_c(0)$ and $W_k(0)$ were initialized to a value of 1.

Because (**SP1**) is a convex problem, we can obtain the solution by differentiating the objective function with $\gamma_k(t)$ for every user as follows:

$$\gamma_k(t) = \Big[\frac{V}{W_k(t)} - 1 \Big]_{\min}^{\max}, \quad \forall k \in \mathcal{K}, \tag{19}$$

where min and max of $\gamma_k(t)$ are design parameters of the system. However, the solution of (**SP2**) is hard to obtain because it is an MINLP which is a combined problem of power allocation and user scheduling of different BSs.

Consequently, the original problem (**P**) is approximated to two subproblems (**P-Pattern**) and (**P1**), and (**P1**) was transformed into (**P2**). Then, it is split into (**SP1**) and (**SP2**). Since the (**SP1**) was solved thanks to its convexity, we propose a low-complex algorithm, namely *CRIM*, in next subsection to solve the remained (**P-Pattern**) and (**SP2**).

B. ALGORITHM DEVELOPMENT

Now, we propose a low-complexity algorithm to solve **(P-Pattern)** and **(SP2)** as shown in Fig. 3. First, we introduce an idea of beam pattern selection probability. It is sparsely updated, e.g., every 100 time slots, to satisfy **(P-Pattern)**. The intuition behind this idea is that variation of path loss in wireless channel is not extremely different for each user within short time, e.g., 0.1 sec. Second, we propose an approximated method to satisfy **(SP2)** by sequentially making decisions of user scheduling, and power allocation.

1) PATTERN-BASED BEAM SELECTION

As mentioned in Section II, we define a set of beam activations. Although the number of possible activated beams is reduced by introducing constraint, finding the set of beam activations every time slot has high computational complexity. Hence, we define the pattern selection probability π_a^n to each BS n, and intermittently change the probability to approximate the activated beam selection procedure. The definition of π_a^n can be as follows:

$$\sum_{a \in \mathcal{A}} \pi_a^n = 1, \quad \forall n \in \mathcal{N}. \tag{20}$$

Then, in a long-time scale, $\boldsymbol{\pi} = \{\pi_a^n\}, \forall a \in \mathcal{A}, \forall n \in \mathcal{N}$ is updated to satisfy **(P-Pattern)** as follows:

(SP-Pattern) :

$$\max_{\boldsymbol{\pi}} \sum_{k \in \mathcal{K}} U_k(R_k) = \sum_{k \in \mathcal{K}} \Big(\sum_{a \in \mathcal{A}} \phi_{k,a} \cdot \pi_a \cdot \bar{r}_{k,a} \Big),$$
$$s.t. \ (20),$$

where $\phi_{k,a} \in [0, 1]$ denotes the probability that the user k is scheduled when the beams in pattern a are activated. In addition, $\bar{r}_{k,a}$ means the average data rate of user k for pattern a during $T_a \gg 1$ time slots. Referring to the concept of [23], standard gradient projection can be applied to determine $\boldsymbol{\pi}$. Therefore, BS n_c computes the partial derivative $D_a^{(n_c)}$ of the utility $U^{(n_c)}$ regarding the activation probability of pattern a

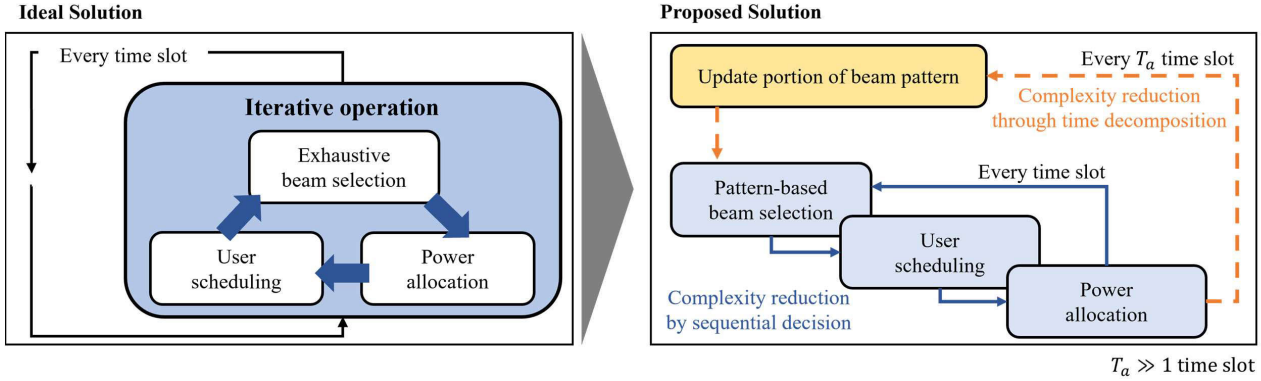

FIGURE 3. The proposed solution with complexity reduction from the ideal solution.

as shown in (21).

$$D_a^{(n_c)} \doteq \frac{\partial U^{(n_c)}}{\partial \pi_a} = \sum_{k \in \mathcal{K}} U_k'(R_k) \cdot \frac{\partial R_k}{\partial \pi_a}, \tag{21}$$

where $\partial R_k/\partial \pi_a = \phi_{k,a}\bar{r}_{k,a} = \bar{\pi}_{k,a}\bar{r}_{k,a}/\pi_a$. Then, the calculation result is transmitted to the MEC server and used to update the $\boldsymbol{\pi}^{n_c}$. Now, each MEC server calculates the probability of beam pattern for each BS by collecting these partial derivatives of the local utility to increase the total network utility as follows:

$$\boldsymbol{\pi} \leftarrow Proj_{\sum_{a \in \mathcal{A}} \pi_a = 1,}(\boldsymbol{\pi} + \beta \boldsymbol{D}). \tag{22}$$

Once π_a^n is decided at long-time scale, each BS n selects beam pattern a with a probability of π_a^n every time slot.

The intuition behind this average-based update is that the average channel gain does not significantly vary for short time. This feature gives a great opportunity to reduce computational complexity by spanning control time scale of beam activation. However, **(SP2)** has an issue of high computational complexity in solving user scheduling and power allocation simultaneously even for given set of beam activations. Hence, we find the solution by sequential decision-making to further reduce the complexity as shown in Fig. 3.

2) USER SCHEDULING AFTER BEAM SELECTION

First, we make a decision of the user scheduling for given set of beam activations. Here, we assume that the transmit power of activated beams is evenly allocated for simplicity. Then, the solution of user scheduling can be obtained by solving **(SP2)** as follows:

$$I_{\boldsymbol{b},k} = \begin{cases} 1, & \text{if} \quad k = k(n, \boldsymbol{b}) \\ & \quad = \arg\max r_k(\boldsymbol{p}_{n,\boldsymbol{b}}) W_k, \\ 0, & \text{otherwise.} \end{cases} \tag{23}$$

Note that the user scheduling problem for given set of beam activations and transmit power is a binary decision problem to satisfy **(SP2)** as shown in equation (23).

3) POWER ALLOCATION AFTER USER SCHEDULING

Each BS allocates transmit power again to users scheduled by (23). However, it requires the entire interfering channel gain information across all activated beams in all BSs. Moreover, the calculation of interference with the entire information also has high computational complexity. Hence, we adopt a heuristic idea to reduce the complexity with a consideration of only one *critical user* as a reference user of which interference approximates the entire interference from all scheduled users in the network.

A critical user is defined as a scheduled user who receives the highest interference from other beams. To select the critical user, we first define two users as follows: *(i)* inner reference user $\text{iru}_{n_c,\boldsymbol{b}}$ who suffers the highest interference from the inner cluster BSs (see (24)), and *(ii)* outer reference user $\text{oru}_{n_c,\boldsymbol{b}}$ who suffers the highest interference from the outer cluster BSs (see (25)). For example, in Fig. 4, the inner and outer reference users of BS 3_1 are indicated in blue- and red-colored arrows, respectively. Then, the critical user $\text{cri}_{n_c,\boldsymbol{b}}$ is designated as a user with the biggest interference among the determined inner and outer reference users (see (26)). Once the critical user is determined, the critical user is representative of all scheduled users to receive the interference.

$$\begin{aligned} \text{iru}_{n_c,\boldsymbol{b}} &= \arg\max |\boldsymbol{h}_{n,k(x,\upsilon^{a_x})}\boldsymbol{b}|^2, \\ &\quad \forall x \in S(n_c), \quad \forall \upsilon^{a_x} \in \mathcal{B}^{a_x}, \end{aligned} \tag{24}$$

$$\begin{aligned} \text{oru}_{n_c,\boldsymbol{b}} &= \arg\max |\boldsymbol{h}_{n,k(y,\upsilon^{a_y})}\boldsymbol{b}|^2, \\ &\quad \forall c' \in \mathcal{C}', \quad \forall y \in E(m_{c'}), \quad \forall \upsilon^{a_y} \in \mathcal{B}^{a_y}, \end{aligned} \tag{25}$$

$$\begin{aligned} \text{cri}_{n_c,\boldsymbol{b}} &= \max(\text{iru}_{n_c,\boldsymbol{b}}, \text{oru}_{n_c,\boldsymbol{b}}), \quad \forall c \in \mathcal{C}, \quad n_c \in \mathcal{N}_c, \\ &\quad b \in \mathcal{B}, \end{aligned} \tag{26}$$

where $S(n_c)$ and $E(m_{c'})$ denote the set of inner cluster BSs except for BS n_c and the set of outer cluster BSs, respectively.

Now, optimal power allocation can be obtained by satisfying KKT (Karush-Kuhn-Tucker) conditions [24] for any user scheduling and critical user selection as follows:

$$p_{k(n_c,\boldsymbol{b})} = \left[\frac{W_{k(n_c,\boldsymbol{b})}/\ln 2}{\lambda_{n_c} + \text{tax}_{n_c,\boldsymbol{b}} + Z_c} - \frac{\eta_{k(n_c,\boldsymbol{b})} + \sigma_{k(n_c,\boldsymbol{b})}}{|\boldsymbol{h}_{n_c,k(n_c,\boldsymbol{b})}\boldsymbol{b}|^2} \right]_0^{P_{n_c}^{\max}}, \tag{27}$$

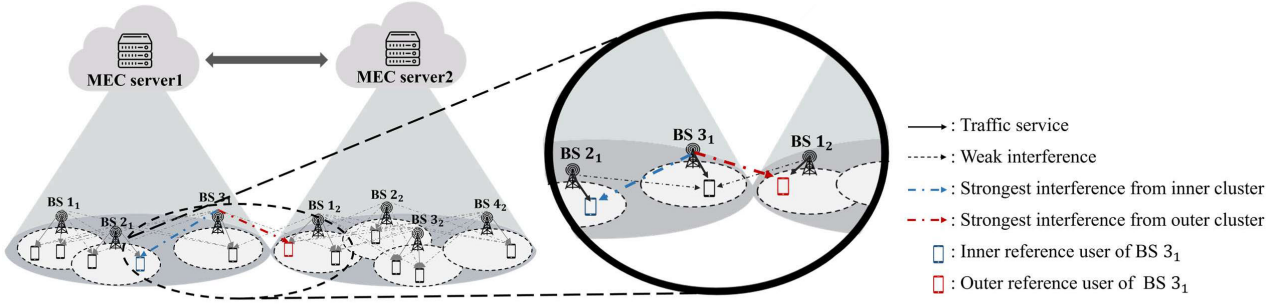

FIGURE 4. The process of critical user selection.

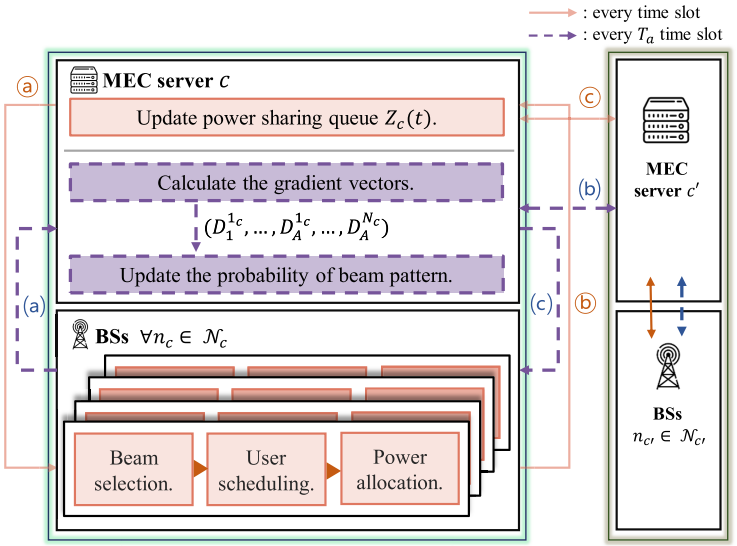

Index	Short-term messages to be exchanged.
ⓐ	Activated beam indices $\mathcal{B}(t)$, scheduled users' indices $\mathcal{K}(t)$, fairness queue W_k, user's RSS of inner cluster, and user's interference plus noise of inner cluster.
ⓑ	Activated beam indices $\boldsymbol{b}(n_c)$, scheduled users' indices $k(n_c, \boldsymbol{b})$, fairness queue W_k, signal strength of all users, and allocated power $p_{n_c,\boldsymbol{b}}$.
ⓒ	Indices of activated beam $\boldsymbol{b}(n_c)$, scheduled users' index $k(n_c)$, and fairness queue $W_{k(n_c)}$.

Index	Long-term messages to be exchanged.
(a)	Partial derivative $D_a^{n_c}$, $\forall a$.
(b)	Avg. RSSs of all users of managing cluster c, and avg. interference plus noise of managing cluster.
(c)	Beam pattern portion of BSs $\pi_a^{n_c}$, avg. RSSs of all users in outer cluster c', and avg. interference plus noise of all users in outer cluster c'.

FIGURE 5. The proposed framework and operation of CRIM algorithm.

where

$$\text{tax}_{n_c,\boldsymbol{b}} = \frac{W_{\text{cri}_{n_c,\boldsymbol{b}}} |\boldsymbol{h}_{n_c,\text{cri}_{n_c,\boldsymbol{b}}} \boldsymbol{b}|^2 \mu_{\text{cri}_{n_c,\boldsymbol{b}}} / \ln 2}{\sum_{v \in \mathcal{N}} \sum_{\boldsymbol{w} \in \mathcal{B}_v} |\sqrt{p_{v,\boldsymbol{w}}} \boldsymbol{h}_{v,\text{cri}_{n_c,\boldsymbol{b}}} \boldsymbol{w}|^2 + \sigma_{\text{cri}_{n_c,\boldsymbol{b}}}}, \tag{28}$$

$$\lambda_{n_c} \Big(\sum_{\boldsymbol{b} \in \mathcal{B}_{n_c}} p_{n_c,\boldsymbol{b}} - P_{n_c}^{\max} \Big) = 0, \tag{29}$$

where $\text{tax}_{n_c,\boldsymbol{b}}$ is designed to impose a penalty on the power allocation. For instance, if a critical user $\text{cri}_{n_c,\boldsymbol{b}}$ suffers high interference from the BS n_c, $\text{tax}_{n_c,\boldsymbol{b}}$ increases as a penalty for it. Due to the strong penalty, $p_{n_c,\boldsymbol{b}}$ would decrease to reduce interference towards the critical user, and vice versa. Now, an initialized positive value λ^{n_c} is updated in the following steps. First, $p_{n_c,\boldsymbol{b}}$ is calculated based on $\text{tax}_{n_c,\boldsymbol{b}}$ and initialized λ^{n_c}. Second, λ_{n_c} is updated according to whether the sum of allocated powers exceeds $P_{n_c}^{\max}$: if exceeds, λ_{n_c} is updated with a higher value to reduce $p_{n_c,\boldsymbol{b}}$ in (27), and vice versa. Next, using updated λ_{n_c}, re-calculate $p_{n_c,\boldsymbol{b}}$. We repeat this operation until the equation (29) satisfies via fast bisection method. In addition, if there is no value of λ_{n_c} that holds the equation (29), then λ_{n_c} becomes zero. Consequently, we obtain the solutions of both **(SP-Pattern)** and **(SP2)**, and the total solution of the problems is called as CRIM algorithm. Now, we summarize what information is exchanged and how CRIM operates on the NOMA-based mmWave network system as illustrated in Fig. 5.

The exchange of all messages in the proposed framework can be summarized as follows (see Fig. 5). First, we can classify the messages into two types. The first type is small-sized messages such as activated beam indices, scheduled user indices, fairness queues and power sharing queues, and the second type is large-sized messages such as the RSS (Received Signal Strength), interference, and thermal noise of all users. In the case of large-sized ones, they can be exchanged among inner cluster BSs in real-time thanks to the short distance between BSs and fast interface (e.g., X2 interface). However, they should be minimally exchanged between clusters due to the long distance between clusters

and slow interface. Hence, small-sized messages can be exchanged in near real-time whereas large-sized messages can be intermittently exchanged with a form of average value.

Then, the inner cluster BSs can exploit all types of messages in real-time whereas the outer cluster BSs can exploit only small-sized ones in real-time, and can intermittently exploit the time-averaged large-sized ones. In other words, the proposed framework exchanges messages as much as possible within the cluster to increase network utility, yet minimally exchanges large-sized ones among inter-clusters to reduce feedback overhead and latency. Since the proposed CRIM algorithm is operated in two different time scales as well, the large-sized messages can be separately exploited in the short time-scale CRIM algorithm (i.e., making a decision of beam pattern) and long time-scale CRIM algorithm (i.e., making decisions of user scheduling and transmit power), respectively.

In the short time-scale (i.e., every time slot t), BS n_c receives small-sized messages ⓐ from server c, and makes decisions of beam activation, user scheduling and transmit power using CRIM as shown in Fig. 5. Then, BS n_c transmits the small-sized ones ⓑ to server c, and the server exchanges the small-sized ones ⓒ among servers in the neighbor clusters. In the long-time scale (i.e., every T_a time slots), BS n_c computes the partial derivative using (21). Then, the calculated partial derivative (a) is sent to server c to update the probability of beam pattern selection $\boldsymbol{\pi}^{n_c}$ as shown in Fig. 5. Then, the large-sized messages (b) are exchanged between servers in the outer clusters, and the large-sized ones (c) are returned to each inner cluster BS.

Algorithm 1 (for every time slot): Each MEC server c receives the abovementioned small-sized messages from the inner cluster BSs. Then, it exchanges small-sized ones with MEC in the outer cluster c'. Once the message exchange is done, the MEC server provides entire messages obtained above to the inner cluster BSs. Next, if the transmit power allocation of BSs is decided, the power sharing queue is updated by the server in the same cluster. Each BS $n_c \in \mathcal{N}_c$ randomly selects the set of beam activations a with probability of $\pi_a^{n_c}$ updated by the MEC server c. Once the set of beam activations is selected, the BS n_c allocates equal transmit power to the selected beams. Then, each BS makes decisions of user scheduling and critical user using (23) and (26), respectively. Then, BS n_c calculates its transmit power using a fast bisection method until $p_{n_c,\boldsymbol{b}}$ converges. Finally, data rates, auxiliary variables and fairness queues for all users are updated.

Algorithm 2 (for every $T_a \gg 1$ time slots): Each MEC server c receives the partial derivative from the BSs $n_c \in \mathcal{N}_c$ to calculate the gradient vector $\boldsymbol{D}$. Then, MEC server c updates the beam pattern selection probability $\boldsymbol{\pi}$ using (22). Moreover, MEC server c exchanges large-sized messages such as time-average RSS and interference plus noises to BSs in the outer cluster during T_a time slots. Thanks to long-time message exchange, the average feedback latency

Algorithm 1 CRIM for Every Time Slot

At each MEC server $\forall c \in \mathcal{C}$,
Receive information from BS n_c :
activated beam indices $\boldsymbol{b}(n_c)(t),\ \forall n_c$.
scheduled users' indices $k(n_c)(t),\ \forall n_c$.
fairness queues $W_{k(n_c)}(t),\ \forall n_c$.
received signal strength $\mathrm{RSS}_{k(n_c)}^{n_c,\boldsymbol{b}},\ \forall n_c,\ \forall b$.
interference plus noise $\omega_{k(n_c)}^{n_c,\boldsymbol{b}} + \sigma_{k(n_c)}^{n_c,\boldsymbol{b}},\ \forall n_c,\ \forall b$.
Send to neighbor MEC server c' :
activated beam indices $\boldsymbol{b}(n_c)(t),\ \forall n_c$.
scheduled users' indices $k(n_c)(t),\ \forall n_c$.
fairness queues $W_{k(n_c)}(t),\ \forall n_c$.
Receive from neighbor MEC server c' :
activated beam indices $\boldsymbol{b}(n_{c'})(t),\ \forall n_{c'} \in \mathcal{N}_{c'},\ \forall c' \in \mathcal{C}'$.
scheduled users' indices $k(n_{c'})(t),\ \forall n_{c'} \in \mathcal{N}_{c'},\ \forall c' \in \mathcal{C}'$.
fairness queues $W_{k(n_{c'})}(t),\ \forall n_{c'} \in \mathcal{N}_{c'},\ \forall c' \in \mathcal{C}'$.
Send to BS n_c :
activated beam indices $\mathcal{B}(t)$, scheduled users' indices $\mathcal{K}(t)$.
fairness queues $W_k(t), \forall k$.
user's received signal strength of inner cluster
$\mathrm{RSS}_{\mathrm{k}(n_c)}^{(x,\nu^{a_x})},\ \forall \nu^{a_x} \in \mathcal{B}^{a_x},\ \forall x \in \mathcal{S}(n_c),\ \forall n_c$.
user's interference plus noise of inner cluster
$\omega_{\mathrm{k}(n_c)}^{(x,\nu^{a_x})} + \sigma_{\mathrm{k}(n_c)}^{(x,\nu^{a_x})},\ \forall \nu^{a_x} \in \mathcal{B}^{a_x},\ \forall x \in \mathcal{S}(n_c),\ \forall n_c$.
power sharing queue $Z_c(t)$.
Receive from BS n_c :
$\boldsymbol{p}_{n_c,\boldsymbol{b}}(t), \forall \boldsymbol{b} \in \mathcal{B}_{n_c}, \forall n_c$ for updating power sharing queue.
Update: power sharing queue $Z_c(t+1)$, using (13).

At each BS $\forall n_c \in \mathcal{N}_c, \forall c \in \mathcal{C}$,
Beam selection: Each BS n_c selects beam pattern a based on probability of beam pattern $\boldsymbol{\pi}^{n_c}$.
Setting initial transmit power: $p_{n_c}^{\boldsymbol{b}}(t) \leftarrow P_{n_c}^{\max}/|\mathcal{B}^{a_n}|$.
User scheduling: Each BS n_c schedules a user using (23) based on selected pattern a.
Send to MEC server c:
activated beam indices $\boldsymbol{b}(n_c)(t)$
scheduled users' indices $k(n_c, \boldsymbol{b})(t)$, fairness queues $W_k(t),\ \forall k$.
received signal strength $\mathrm{RSS}_{k(n_c)}^{(n_c,\boldsymbol{b})},\ \forall k$.
interference plus noise $\omega_{k(n_c)}^{(n_c,\boldsymbol{b})} + \sigma_{k(n_c)}^{(n_c,\boldsymbol{b})},\ \forall k$.
Receive from MEC server c:
activated beam indices $\mathcal{B}(t)$, scheduled users' indices $\mathcal{K}(t)$.
Inner cluster scheduled users' received signal strength
$\mathrm{RSS}_{k(x,\nu^{a_x})}^{(n_c,\boldsymbol{b})},\ \forall x \in S(n_c),\ \forall \nu^{a_x} \in \mathcal{B}^{a_x}$.
Inner cluster scheduled users' interference plus noise
$\omega_{k(x,\nu^{a_x})}^{(n_c,\boldsymbol{b})} + \sigma_{k(x,\nu^{a_x})}^{(n_c,\boldsymbol{b})},\ \forall x \in S(n_c),\ \forall \nu^{a_x} \in \mathcal{B}^{a_x}$.
fairness queues from inner and outer cluster scheduled users,
$W_{k(x)}, \forall x \in S(n_c)$ and $W_{k(y)}, \forall y \in S(n_{c'})$, respectively.
power sharing queue $Z_c(t)$.
Critical user selection: Determine the critical user from inner and outer reference users (26).
Power allocation:
$[i, j] \leftarrow [0, \lambda_{n_c}^{max}]$.
while $|\sum_{\boldsymbol{b} \in \mathcal{B}_{n_c}} p_{n_c,\boldsymbol{b}}(t) - P_{n_c}^{max}| < \delta$ **do**
Set $\lambda_{n_c} = (i+j)/2$ and update $p_{n,\boldsymbol{b}}(t)$ using (27).
if $\sum_{\boldsymbol{b} \in \mathcal{B}_n} p_{n,\boldsymbol{b}}(t) > P_{n_c}^{max}$ **then**
$[i, j] \leftarrow [\lambda_{n_c}, j]$.
else if $\sum_{\boldsymbol{b} \in \mathcal{B}_n} p_{n,\boldsymbol{b}}(t) < P_{n_c}^{max}$ **then**
$[i, j] \leftarrow [i, \lambda_{n_c}]$.
end if
end while.
Update: $r_k(t),\ \gamma_k(t)$, and $W_k(t+1), \forall k \in \mathcal{K}_{n_c}$
using (10), (19), and (14), respectively.
Send to MEC server c : $\boldsymbol{p}_{n_c}(t)$ for updating power sharing queue.

Algorithm 2 CRIM for Every $T_a \gg 1$ Time Slots

At each MEC server $\forall c \in \mathcal{C}$**,**
Calculate gradient vector: MEC server computes the gradient vector $\boldsymbol{D}^{\boldsymbol{n_c}} = (D_1^{n_c}, \cdots, D_A^{n_c})$ by collecting $D_a^{n_c}$.
Update pattern portion: MEC server updates the probability of beam pattern $\boldsymbol{\pi}$ using (22).
Send to neighbor MEC server c' :
avg. RSSs of all associated users in cluster c
$\overline{\text{RSS}_k^{n_c,\boldsymbol{b}}}, \forall k \in \mathcal{K}_{n_c},\ \forall \boldsymbol{b} \in \mathcal{B}_{n_c},\ \forall n_c.$
avg. interference plus noise of all associated users in cluster c
$\overline{\omega_k^{n_c,\boldsymbol{b}} + \sigma_k^{n_c,\boldsymbol{b}}},\ \forall k \in \mathcal{K}_{n_c},\ \forall \boldsymbol{b} \in \mathcal{B}_{n_c},\ \forall n_c.$
Receive from neighbor MEC server c' :
avg. RSS of all users in outer clusters
$\overline{\text{RSS}_k^{m_{c'},\boldsymbol{b}}}, \forall k \in \mathcal{K}_{m_{c'}},\ \forall \boldsymbol{b} \in \mathcal{B}_{m_{c'}}, \forall m_{c'} \in \mathcal{N}_{c'},\ \forall c' \in \mathcal{C}'.$
avg. interference plus noise of all users in outer clusters
$\overline{\omega_k^{m_{c'},\boldsymbol{b}} + \sigma_k^{m_{c'},\boldsymbol{b}}}, \forall k \in \mathcal{K}_{m_{c'}}, \forall \boldsymbol{b} \in \mathcal{B}_{m_{c'}}, \forall m_{c'} \in \mathcal{N}_{c'}, \forall c' \in \mathcal{C}'.$
Send to BS n_c :
beam pattern portion of BSs $\pi_a^{n_c},\ \forall a \in \mathcal{A}, \forall n_c$
avg. RSSs of all users in BSs in outer clusters
$\overline{\text{RSS}_k^{m_{c'},\boldsymbol{b}}}, \forall k \in \mathcal{K}_{m_{c'}},\ \forall \boldsymbol{b} \in \mathcal{B}_{m_{c'}}, \forall m_{c'} \in \mathcal{N}_{c'},\ \forall c' \in \mathcal{C}'.$
avg. interference plus noise of all users in BSs in outer clusters
$\overline{\omega_k^{m_{c'},\boldsymbol{b}} + \sigma_k^{m_{c'},\boldsymbol{b}}}, \forall k \in \mathcal{K}_{m_{c'}}, \forall \boldsymbol{b} \in \mathcal{B}_{m_{c'}}, \forall m_{c'} \in \mathcal{N}_{c'}, \forall c' \in \mathcal{C}'.$

At each BS $\forall n_c \in \mathcal{N}_c, \forall c \in \mathcal{C}$**,**
Calculate partial derivative c :
computes the partial derivative $D_a^{n_c}$ using (21). $\forall a \in \mathcal{A}$.
Send to MEC server c : partial derivative $D_a^{n_c}$. $\forall a \in \mathcal{A}$.
Receive from MEC server c :
avg. RSS of users in BSs in outer clusters
$\overline{\text{RSS}_k^{m_{c'},\boldsymbol{b}}}, \forall k \in \mathcal{K}_{m_{c'}},\ \forall \boldsymbol{b} \in \mathcal{B}_{m_{c'}}, \forall m_{c'} \in \mathcal{N}_{c'},\ \forall c' \in \mathcal{C}'.$
avg. interference plus noise of users in BSs in outer clusters
$\overline{\omega_k^{m_{c'},\boldsymbol{b}} + \sigma_k^{m_{c'},\boldsymbol{b}}}, \forall k \in \mathcal{K}_{m_{c'}}, \forall \boldsymbol{b} \in \mathcal{B}_{m_{c'}}, \forall m_{c'} \in \mathcal{N}_{c'}, \forall c' \in \mathcal{C}'.$

and overhead between servers can be further reduced and the CRIM algorithm can be practically operated.

IV. PERFORMANCE EVALUATION

In this section, we evaluate the proposed CRIM algorithm and existing algorithms via simulations with the realistic channel model and parameters in 5G standard [25].

A. SETUP

For the wireless channel model, we use UMi-street canyon pathloss model with 28GHz of center frequency (mmWave) [25]. In our simulation scenarios, each BS is assumed to have 10 transmit antennas, and the maximum transmit power of each BS and long-term transmit power budget of each cluster are set to 2W and 1W multiplied by the number of BSs included in each cluster, respectively. We carry out the simulations based on the real BS topology in South Korea to see the GAT performance of algorithms. In addition, to show the different impact of various parameters on the system performance, positions of BSs are stochastically generated by PPP (Poisson point process) model [26] which captures the realistic heterogeneity of the cellular networks.[8] For all simulation scenarios, 4 clusters are considered, and we manually locate each cluster so as to contain a similar number of BSs.[9] Moreover, each user belongs to a single BS, and the positions of each users are randomly determined. The total operation time of each simulation is set to 5000 time slots where each time slot is set to 1 millisecond.

We compare the existing algorithms, i.e., *Greedy* [27], *IGS* [28], and *ON/OFF* [29] with CRIM. In the Greedy algorithm, each user selects a beam greedily so as to achieve the highest SINR in conjunction with proportional fairness (PF) scheduling policy. Next, the IGS algorithm selects user and beam pairs sequentially. When selecting each pair, the user selects a beam that can achieve the highest SINR with a consideration of the interference from the previously selected pairs. The ON/OFF algorithm is designed based on the 3GPP standard [29]. First, users are scheduled according to the PF scheduling policy assuming that all beams in all BSs are activated. Next, each BS checks whether the strength of interference to users scheduled in other BSs is higher than the pre-defined threshold or not. If the interference is larger than the threshold, then the corresponding BS is deactivated, vice versa.

To compare the existing algorithms with CRIM, we consider three metrics: GAT (Geometric Average user Throughput), Avg. throughput (Average user Throughput), and allocated power. Maximizing the GAT (in Mbps) is equivalent to maximizing our objective value, i.e., **(P)** meaning that it takes into account both fairness and throughput of users. The Avg. throughput (in Mbps) is time average throughput of users in the entire network. The allocated power (in Watt) is the amount of transmit power allocated to the scheduled user.

On top of this setup, we conduct four simulations as follows: *(i)* simulation on the real network topologies in South Korea, *(ii)* simulation for different BS intensities in PPP model, *(iii)* simulation for different the average number of users in each BS in PPP model, and *(iv)* simulation for different multiple access schemes on CRIM in PPP model. Via simulations, we could observe interesting points as follows: *(i)* CRIM outperforms the existing algorithms in terms of GAT and Avg. throughput, *(ii)* the impact of spatio-temporal power sharing is significant, and *(iii)* the advantage of NOMA is more pronounced in CRIM than in the existing algorithms. We describe these observations in detail as follows.

First, we compare the GAT performance of CRIM and the existing algorithms on the real network topologies deployed in the metropolitan area of South Korea. As depicted in Fig. 6, two network topologies are considered and named as *Seoul*1 and *Seoul*2. Each topology has 25 and 21 BSs, respectively, with 4 clusters positioned to contain 4 to 7 BSs. As shown in Fig. 7, it can be confirmed that CRIM outperforms the existing algorithms in terms of GAT for both topologies. For

[8] In this model, we define the average number of BSs in the network as the intensity.

[9] Note that the optimization of clustering BSs can be considered as another research issue, but it is out of scope of this paper.

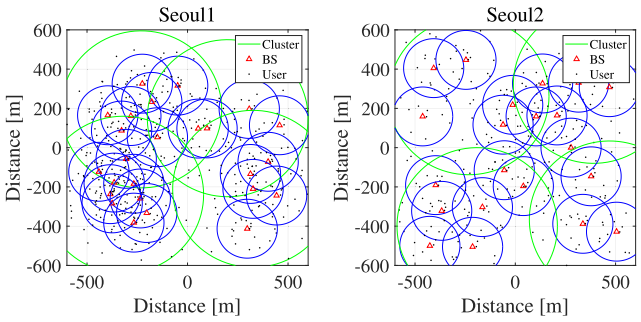

FIGURE 6. The real network topology in South Korea.

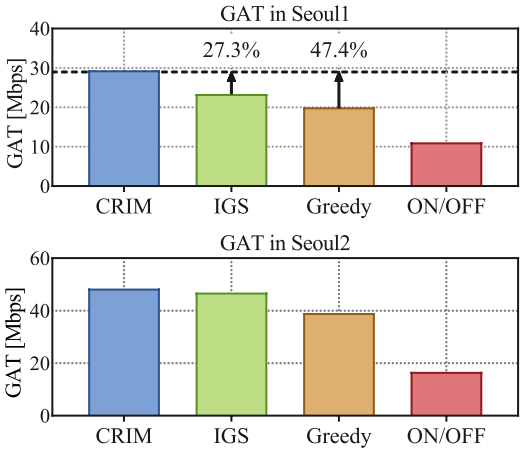

FIGURE 7. GAT for different network topologies.

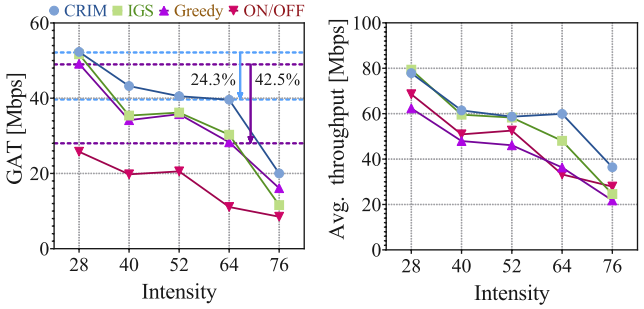

FIGURE 8. Performance comparison for different intensities.

example, in *Seoul* 1, the GAT improvements from the existing algorithms to CRIM are 27.3% (in IGS), 47.4% (in Greedy) and 164.9% (in ON/OFF).

B. THROUGHPUT PERFORMANCE

C. IMPACT OF SPATIAL POWER SHARING

To see the impact of spatial power sharing that shares transmit power within the same cluster, simulations are conducted while increasing the intensity of BSs in PPP model. As the intensity increases, the distances between the BSs decrease, which results in greater interference to users. Fig. 8 shows that the performance of all algorithms decreases when intensity becomes higher. However, in the case of CRIM, it can be

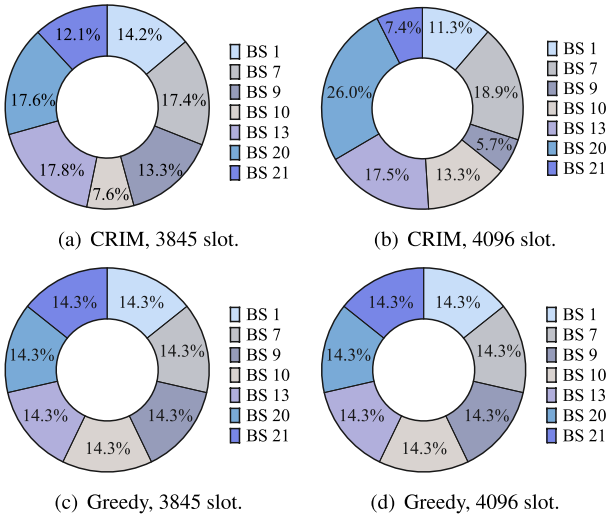

FIGURE 9. Ratio of transmit powers of BSs in cluster 2.

seen that the performance degradation is smaller than that of the other algorithms. In aspects of fairness, BSs have to allocate more transmit power to edge users who suffer more interference when intensity increases. If BSs use a fixed transmit power budget (i.e., other algorithms), center users will be allocated less transmit power inevitably. On the contrary, CRIM can exploit spatial power sharing to share transmit power among BSs in the same cluster while keeping the average transmit power constraint. Moreover, Fig. 9 shows the ratio of transmit power usage of each BS included in cluster 2 in case of CRIM and Greedy. As shown in Fig. 9(a) and Fig. 9(b), the results show that CRIM differently allocates transmit power to BSs in different time slots. In other words, if higher transmit powers in BSs are allocated in previous time slots, then lower transmit powers in the BSs are allocated in future time slots, and vice versa. On the other hand, in Fig. 9(c) and Fig. 9(d), the results depict that Greedy allocates the same transmit powers in BSs for both time slots.

D. IMPACT OF TEMPORAL POWER SHARING

We conduct simulations to observe GAT performance as a function of the average number of users. For the simulation topology, 4 clusters and 7 BSs at each cluster are deployed according to the PPP model. As shown in Fig. 10, the performance degradation of CRIM is smaller than that of the other algorithms as the average number of users increases. This is because CRIM can exploit the degree of freedom for temporal power sharing, which flexibly uses a certain amount of transmit power budget for long-time period. Fig. 11 depicts the transmit power allocated to users scheduled in a certain BS (i.e., BS 2) for selected time slots[10] when the average number of users is set to be 12 and 20, respectively, and user indices of legend are assigned in

[10]We select these time slots randomly.

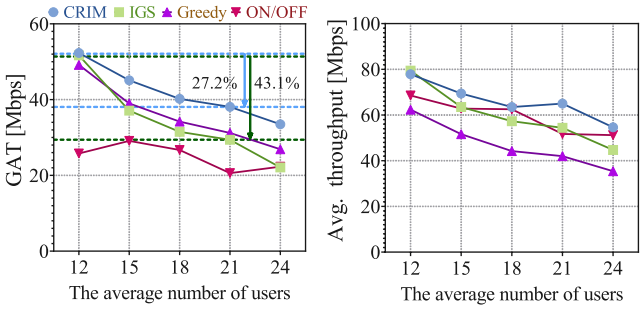

FIGURE 10. Performance comparison for different the average number of users.

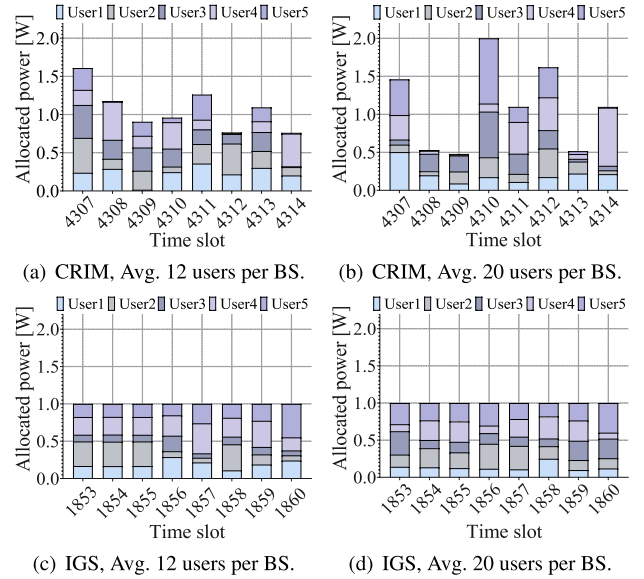

FIGURE 11. Allocated transmit power to users for selected time slots for different the average number of users in BS 2.

order of distance from the BS. As shown in Fig. 11(a) and Fig. 11(b), CRIM takes advantage of temporal power sharing, and as the number of users increases, CRIM uses more transmit power to edge users than fewer users without significant reduction of transmit power allocated to other users. On the other hand, in Fig. 11(c) and Fig. 11(d), IGS uses the same transmit power budget (1W) and decreases transmit power allocated to center users to allocate more transmit power to edge users as the average number of users increases.

E. IMPACT OF DIFFERENT PHY TECHNOLOGIES

We compare the GAT performance of CRIM for different multiple access schemes, i.e., OFDMA and NOMA as shown in Fig. 12. When the OFDMA scheme is applied, if users are scheduled in the same beam, the system channel bandwidth is divided to be orthogonal for each user. Thanks to the orthogonal system channel bandwidth, intra-beam interference can be ignored. However, the average data rate becomes smaller in proportion to the number of users scheduled in

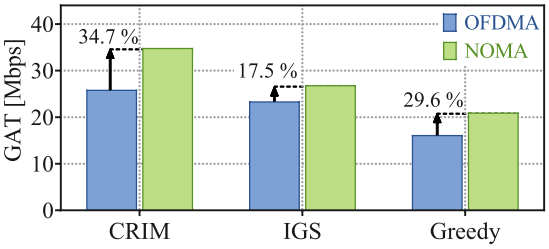

FIGURE 12. GAT for different multiple access schemes.

same beam due to the divided system channel bandwidth. On the other hand, when the NOMA scheme is applied, if users are scheduled in the same beam, intra-beam interference can be reduced by leveraging SC and SIC techniques. Moreover, there is no concern about the degradation of data rate as the system channel bandwidth is not divided for different resource blocks. Because of this, CRIM can obtain approximately 35% of performance increment in NOMA than in OFDMA. Moreover, since the spatio-temporal degree of freedom is greater in CRIM than that in other algorithms, we can see that the performance increment of CRIM from OFDMA to NOMA is better than the other algorithms.

V. CONCLUSION

In this paper, we proposed a low-complex beam activation, user scheduling, and power allocation algorithm for network utility maximization. To reduce the computational complexity of the original problem, we introduced several heuristic but practical methods which approximate our problem with low complexity: *(i)* time scale decomposition, *(ii)* sequential decision making of beam activation, use scheduling and power allocation, and *(iii)* abstraction of interference into a single critical user. These methods are likely to be tailored to a future network architecture where small BSs are managed by a single MEC server and the MEC server can manage transmit power budget in real-time. Via realistic simulations, we verified that the proposed CRIM algorithm outperforms the existing algorithms by showing 47.4% better utility performance. We believe that the design of low-complex and practical algorithms which exploit the different characteristics of the novel network architecture would be pervasive in the future.

ACKNOWLEDGMENT

An earlier version of this paper was presented in part at the ICOIN 2022 [30].

REFERENCES

[1] (Mar. 2020). *Cisco Annual Internet Report (2018–2023).* Cisco Public White Paper. [Online]. Available: https://www.cisco.com/c/en/us/solutions/collateral/executive-perspectives/annual-internet-report/white-paper-c11-741490.pdf

[2] S. A. Busari, K. M. S. Huq, S. Mumtaz, L. Dai, and J. Rodriguez, "Millimeter-wave massive MIMO communication for future wireless system: A survey," *IEEE Commun. Surveys Tuts.*, vol. 20, no. 2, pp. 836–869, 2nd Quart., 2017.
[3] J. Kim, H.-W. Lee, and S. Chong, "Virtual cell beamforming in cooperative networks," *IEEE J. Sel. Areas Commun.*, vol. 32, no. 6, pp. 1126–1138, Jun. 2014.
[4] M. Kamel, W. Hamouda, and A. Youssef, "Ultra-dense networks: A survey," *IEEE Commun. Surveys Tuts.*, vol. 18, no. 4, pp. 2522–2545, 4th Quart., 2016.
[5] (Jul. 2014). *5G Radio Access: Requirements Concept and Technologies*. DOCOMO 5G White Paper. [Online]. Available: https://www.docomo.ne.jp/english/binary/pdf/corporate/technology/whitepaper_5g/DOCOMO_5G_White_Paper.pdf
[6] C. Liu, M. Li, S. V. Hanly, P. Whiting, and I. B. Collings, "Millimeter-wave small cells: Base station discovery, beam alignment, and system design challenges," *IEEE Wireless Commun.*, vol. 25, no. 4, pp. 40–46, Aug. 2018.
[7] J. Liu, M. Sheng, L. Liu, and J. Li, "Interference management in ultra-dense networks: Challenges and approaches," *IEEE Netw.*, vol. 31, no. 6, pp. 70–77, Nov. 2017.
[8] J. Xiao, C. Yang, A. Anpalagan, Q. Ni, and M. Guizani, "Joint interference management in ultra-dense small-cell networks: A multi-domain coordination perspective," *IEEE Trans. Commun.*, vol. 66, no. 11, pp. 5470–5481, Nov. 2018.
[9] C. Liu, M. Li, S. V. Hanly, and P. Whiting, "Joint downlink user association and interference management in two-tier HetNets with dynamic resource partitioning," *IEEE Trans. Veh. Technol.*, vol. 66, no. 2, pp. 1365–1378, Feb. 2017.
[10] J. Cui, Y. Liu, Z. Ding, P. Fan, and A. Nallanathan, "Optimal user scheduling and power allocation for millimeter wave NOMA systems," *IEEE Trans. Wireless Commun.*, vol. 17, no. 3, pp. 1502–1517, Mar. 2017.
[11] Y. Song and S. Xu, "Beam management based multi-cell interference suppression for millimeter wave communications," in *Proc. IEEE 93rd Veh. Technol. Conf. (VTC-Spring)*, Apr. 2021, pp. 1–5.
[12] Y.-X. Zhu, D.-Y. Kim, and J.-W. Lee, "Joint antenna and user scheduling in the massive MIMO system over time-varying fading channels," *IEEE Access*, vol. 9, pp. 92431–92445, 2021.
[13] Z. Chen, Z. Ding, X. Dai, and R. Zhang, "An optimization perspective of the superiority of noma compared to conventional OMA," *IEEE Trans. Signal Process.*, vol. 65, no. 19, pp. 5191–5202, Oct. 2017.
[14] A. Nasser, O. Muta, M. Elsabrouty, and H. Gacanin, "Interference mitigation and power allocation scheme for downlink MIMO-NOMA HetNet," *IEEE Trans. Veh. Technol.*, vol. 68, no. 7, pp. 6805–6816, Jul. 2019.
[15] F. Fang, H. Zhang, J. Cheng, and V. C. M. Leung, "Energy-efficient resource allocation for downlink non-orthogonal multiple access network," *IEEE Trans. Commun.*, vol. 64, no. 9, pp. 3722–3732, Sep. 2016.
[16] J. Kwak, L. B. Le, G. Iosifidis, K. Lee, and D. I. Kim, "Collaboration of network operators and cloud providers in software-controlled networks," *IEEE Netw.*, vol. 34, no. 5, pp. 98–105, Sep. 2020.
[17] J. Hong, Y. Cho, S. Kim, J. Na, and J. Kwak, "Spatio-temporal degree of freedom: Interference management in 5G edge SON networks," in *Proc. ICOIN*, Jan. 2021, pp. 1–3.
[18] L. Jorguseski, A. Pais, F. Gunnarsson, A. Centonza, and C. Willcock, "Self-organizing networks in 3GPP: Standardization and future trends," *IEEE Commun. Mag.*, vol. 52, no. 12, pp. 28–34, Dec. 2014.
[19] M. J. Neely, "Stochastic network optimization with application to communication and queueing systems," *Synth. Lectures Commun. Netw.*, vol. 3, no. 1, pp. 1–211, Jan. 2010.
[20] E. Kim, J. Kwak, and S. Chong, "Exception of dominant interfering beam: Low complex beam scheduling in mmWave networks," in *Proc. WCNC*, Seoul South Korea, Jun. 2020, pp. 25–28.
[21] A. Goldsmith, *Wireless Communications*. Cambridge, U.K.: Cambridge Univ. Press, 2005.
[22] J. Mo and J. Walrand, "Fair end-to-end window-based congestion control," *IEEE/ACM Trans. Netw.*, vol. 8, no. 5, pp. 556–567, Oct. 2000.
[23] K. Son, Y. Yi, and S. Chong, "Utility-optimal multi-pattern reuse in multi-cell networks," *IEEE Trans. Wireless Commun.*, vol. 10, no. 1, pp. 142–153, Jan. 2011.
[24] S. Boyd, *Convex Optimization*. Cambridge, U.K.: Cambridge Univ. Press, 2004.
[25] *Study on Channel Model for Frequency Spectrum Above 6 GHz; (Release 14)*, Standard 3GPP TR 38.900, Jun. 2016. [Online]. Available: https://www.3gpp.org/release-14
[26] R. Streit, *The Poisson Point Process*. Cham, Switzerland: Springer, 2010.
[27] R. Pal, A. K. Chaitanya, and K. V. Srinivas, "Low-complexity beam selection algorithms for millimeter wave beamspace MIMO systems," *IEEE Commun. Lett.*, vol. 23, no. 4, pp. 768–771, Apr. 2019.
[28] Z. Jiang, S. Chen, S. Zhou, and Z. Niu, "Joint user scheduling and beam selection optimization for beam-based massive MIMO downlinks," *IEEE Trans. Wireless Commun.*, vol. 17, no. 4, pp. 2190–2204, Apr. 2018.
[29] *Study on Small Cell Enhancements for E-UTRA and E-UTRAN Physical-Layer Aspects; (Release 12)*, Standard 3GPP TR 36.872, Dec. 2013. [Online]. Available: https://www.3gpp.org/release-12
[30] S. Ahn, J. Hong, Y. Cho, J. Na, and J. Kwak, "Sequential beam, user, and power allocation for interference management in 5G mmWave networks," in *Proc. Int. Conf. Inf. Netw. (ICOIN)*, Jan. 2022, pp. 1–6.

JOONPYO HONG (Student Member, IEEE) received the B.S. degree in IT convergence from Soongsil University, Seoul, South Korea, in 2019, and the M.S. degree in electrical engineering and computer science from DGIST, Daegu, South Korea, in 2022. His research interests include hybrid SON architecture and the practical interference management in small cell networks and optimizing resource allocation for 5G cellular networks.

PILDO YOON (Student Member, IEEE) received the B.S. degree in computer engineering from Hanbat National University, Daejeon, South Korea, in 2022. He is currently pursuing the master's degree with DGIST, Daegu, South Korea. His research interests include the practical interference management in heterogeneous cellular networks and resource optimization on cellular network via reinforcement learning.

SUYOUNG AHN (Student Member, IEEE) received the B.S. degree in electronic engineering from Daegu University, Gyeongsan-si, South Korea, in 2020, and the M.S. degree in electrical engineering and computer science from DGIST, Daegu, South Korea, in 2022. Her research interests include the areas of interference management in cellular networks and reinforcement learning.

YUNHEE CHO received the M.S. and Ph.D. degrees from the Department of Electrical Engineering, Korea Advanced Institute of Science and Technology (KAIST), Daejeon, South Korea, in 2001 and 2014, respectively. Since 2001, she has been with the Electronics and Telecommunications Research Institute (ETRI), Daejeon, where she is currently a Principal Researcher. Her research interests include 4G, 5G small cells, self-organizing networks (SON), compact MIMO, beamforming, interference management of multi-cell OFDMA networks, quality of experience (QoE), and universal access of HetNet.

JEEHYEON NA (Member, IEEE) received the B.S. degree in computer science from Chonnam National University, and the M.S. and Ph.D. degrees in computer science from Chungnam National University, in 2002 and 2008, respectively. She has been with the Electronics and Telecommunications Research Institute (ETRI), since 1989, where she is currently the Director of the Intelligent Ultra Dense Small Cell Research Section. Her research interests include the area of 4G, 5G small cells, self-organizing networks (SON), and location management and paging for mobile communication networks. She is a member of IEICE Communication Part.

JEONGHO KWAK (Member, IEEE) received the B.S. degree (summa cum laude) in electrical and computer engineering from Ajou University, Suwon, South Korea, in 2008, and the M.S. and Ph.D. degrees in electrical engineering from KAIST, Daejeon, South Korea, in 2011 and 2015, respectively. He is currently an Assistant Professor with the Department of Electrical Engineering and Computer Science, DGIST, Daegu, South Korea. Prior to joining DGIST, he was with INRS-EMT, Montreal, Canada, and Trinity College Dublin, Dublin, Ireland, as a Postdoctoral Researcher and a Marie Sklodowska-Curie Fellow, respectively. His current research interests include learning model & resource allocation in hybrid cloud/edge network architecture, energy optimization in heterogeneous networks, and radio resource management for 6G wireless cellular/satellite networks.